Conference Paper

Deciphering Astroglial Dynamics and Interactions Through Multi-Scale Computational Modeling in Multiple Sclerosis Evolution

Chrysoula Tsimperi[1,*], Konstantinos Michmizos[2] and Leontios Hadjileontiadis[1]

[1] Department of Electrical and Computer Engineering, Aristotle University of Thessaloniki, Thessaloniki, Greece.
[2] Computational Brain Lab, Department of Computer Science, Rutgers University, Piscataway, NJ, United States.

[*] Corresponding Author Email: xrysa97.tsiberi@gmail.com

ABSTRACT

Multiple sclerosis (MS) is a neurodegenerative disease affecting millions worldwide, highlighting the complex relationship between the immune system and the central nervous system. Astrocytes are recognized as significant contributors to the disease's pathogenesis. In this work, a biophysically realistic astrocytic model was created to investigate astrocytes' role in MS development, focusing on their impact on axonal conduction and enhanced sodium channel facilitation in demyelinated axons. Through the advancement of comprehension about the involvement of astrocytes in the pathophysiology of MS, this study explores the processes underlying the disease. The study also examines the morphology of astrocytes and its influence on cellular activity, providing insights into cell instability drivers and the interaction between morphological changes and functional modifications. This approach aims to understand the complex connections between cellular characteristics and physiological attributes, enhancing our understanding of multiple sclerosis and potentially developing groundbreaking therapies.

Keywords—*Astrocytes, Conduction velocity, In-Silico, Multiple sclerosis.*

INTRODUCTION

Astrocytes are key contributors to multiple sclerosis (MS) lesions, playing a crucial role in maintaining neural homeostasis and preventing neural tissue damage.[1] They exhibit dual roles, responding adaptively or non-adaptively to the severity of injury.[2,3] Their intricate morphology and adaptive responses are central to MS lesion development.[4,5] However, this dual nature, providing both protection and potential hindrance, makes them complex therapeutic targets.[6] In this study, our primary objective is to delve into the role of astrocytes in the development of MS lesions, adopting a comprehensive approach through three distinct parts. The first part explores how astrocytes influence axonal conduction, with implications for MS-related functional deficits. The second part examines how astrocytes facilitate sodium channels in demyelinated axons, shedding light on potential MS pathophysiology mechanisms. The third part seeks to correlate the loss and recovery of astrocytes in the cerebral cortex with myelin loss due to conduction block in new MS lesions. Our approach involves creating biologically realistic models of two distinct astrocytic states, one representing physiological conditions and the other mimicking pathological scenarios. These models serve as the foundation for our study, enabling us to expand our understanding of various factors, including demyelinated and remyelinated axon conductance, the role of ions as signaling molecules (such as Ca^{2+}, Na^{+}, and K^{+}), and the impact of inflammatory cytokines like IL1β/6 and TNFα . Our overarching goal is to develop comprehensive computational representations of astrocytes that encompass both their physiological and pathological behaviors within the neocortex area. By developing biophysically realistic models and incorporating empirical data, we aim to accurately capture astrocyte morphology and functionality while exploring their behavior across different scales.

METHODS

In this study, we aimed to unravel the intricate machinery underlying astroglial pathophysiology in MS by addressing the challenge of their complex, sponge-like morphology. This work systematically assessed the multiscale morphology of astroglia to create a realistic multicompartment cell model for biophysical interrogation within the NEURON computational environment. As a proof of concept, we simulated two neocortex astrocytes in a virtual environment, subjecting them to a series of imaging experiments. This allowed us to reveal crucial aspects of astroglial pathophysiology that are challenging to access through empirical methods. These findings encompassed spatiotemporal dynamics of intracellular K^{+} and Na^{+} redistribution, essential Ca^{2+} buffering properties, as well as the effects of demyelinated and remyelinated axon conductance and the influence of inflammatory cytokines such as IL1β/6 and TNFα. We aimed to create a modeling approach that faithfully replicates the intricate morphology of astrocytes across multiple scales while retaining the full capabilities of biophysical simulations provided by NEURON.

A. Significance of Morphology in MS

Brain astroglia has a distinct morphology compared to nerve cells due to their complex system of nanoscopic processes that fill tissue volume between branches.[3,7] They are often seen as a cloudy structure around thicker branches and do not overlap in tissue domains.[8,9] In MS lesions, astroglia plays complex roles, influencing inflammation and neuronal repair. The nervous system influences the shapeshifting properties of reactive astrocytes, which can be influenced by damage severity. Traumatic brain injuries can increase GFAP levels, leading to cell-body hypertrophy and hot spots of cell proliferation (Figure 1). The presence of astrocytes near focal lesions can lead to "palisades" and decreased astrogliosis hallmarks.[3,10,11]

To develop effective therapies targeting astrocytes, a deeper understanding of their subtypes and functions is essential. Super-resolution imaging techniques hold promise in unraveling astrocyte behavior in MS.[12] Due to the varying cellular mechanisms and morphological features of astroglia, it is important to develop a model that can explore astroglial functions under pathological conditions.

B. Data Selection

In this study, we employed a multifaceted approach to investigate the role of cortical astrocytes in the context of neocortical lesions associated with MS. Using datasets from mouse models, we harnessed advanced imaging

techniques to visualize the intricate morphological changes of astrocytes within the cortex when neocortical lesions are present. For this work, it was selected two datasets of astrocytes (physiology and pathophysiology) from the neocortex area from the NEUROMORPHO database (Tables 1 and 2) for the development of an interactive realistic model.[13]

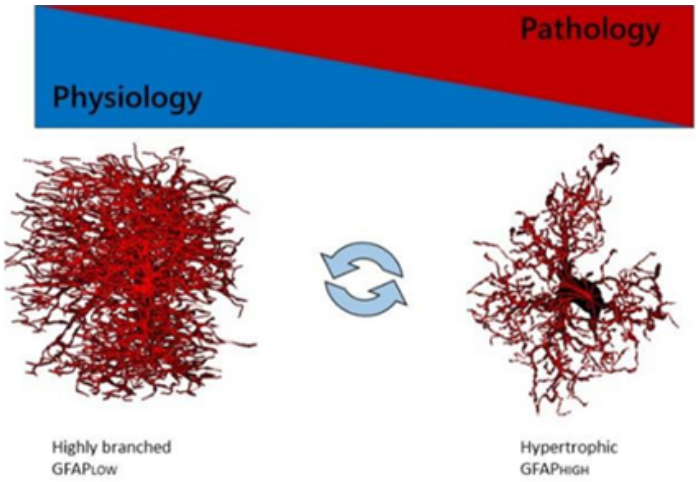

FIGURE 1. Function of the Astrocyte from Homeostasis to Pathology.

TABLE 1. Measurements of physiology cell.

Measurements	Data
Soma Surface	67.05 μm^2
Number of Stems	13
Number of Bifurcations	742
Number of Branches*	1497
Overall Width	44.67 μm
Overall Height	52.97 μm
Overall Depth	51.07 μm
Average Diameter	0.51 μm
Total Length	8281.73 μm
Total Surface**	11237.8 μm^2
Total Volume**	2672.6 μm^3
Max Euclidean Distance	41.74 μm
Max Path Distance	63.29 μm
Max Branch Order	27
Average Contraction	0.87
Total Fragmentation	7466
Partition Asymmetry	0.65
Average Rall's Ratio	1.9
Average Bifurcation Angle Local	65.21°
Average Bifurcation Angle Remote	77.33°
Fractal Dimension	1.1

* Rows highlighted in blue represent the number of branches.

** Rows highlighted in red correspond to surface area and volume parameters, which are utilized in calculating the surface-to-volume ratio (SVR).

TABLE 2. Measurements of pathology cell.

Measurements	Data
Soma Surface	126.98 μm^2
Number of Stems	6
Number of Bifurcations	267
Number of Branches*	540
Overall Width	24.57 μm
Overall Height	67.02 μm
Overall Depth	51.54 μm
Average Diameter	0.64 μm
Total Length	3160.88 μm
Total Surface**	5575.83 μm^2
Total Volume**	2820.8 μm^3
Max Euclidean Distance	46.74 μm
Max Path Distance	62.2 μm
Max Branch Order	26
Average Contraction	0.83
Total Fragmentation	3764
Partition Asymmetry	0.62
Average Rall's Ratio	2.08
Average Bifurcation Angle Local	69.86°
Average Bifurcation Angle Remote	75.01°
Fractal Dimension	1.11

* Rows highlighted in blue represent the number of branches.

** Rows highlighted in red correspond to surface area and volume parameters, which are utilized in calculating the surface-to-volume ratio (SVR).

C. Incorporation of Astrocyte Mechanisms

This section discusses the versatility of models built, emphasizing their ability to incorporate numerous NEURON-enabled channel and transporter kinetic mechanisms validated through experiments and simulations. Formal descriptions of these algorithms are accessible through the extensive NEURON database, SenseLab. The model includes various channel current and diffusion-reaction mechanisms tailored to this study. These mechanisms encompass the Kir4.1 potassium current, intracellular K^+ and Na^+ diffusion, the demyelination and remyelination axon conductance mechanism, and K^+/Na+ extrusion.[14, 15] Gap junction mechanisms are also incorporated, offering options for current leakage or diffuse escape.[8] Also, we delve into the simulation algorithms that govern intracellular Ca^{2+} dynamics in MSASTRO, including the diffusion of Ca^{2+} among compartments of different sizes. These algorithms draw from NEURON Book 24 and are adapted from the modified cadifus.mod file.[16]

D. Generating Complete Astrocyte Morphology

The study's methods involved setting up the NEURON environment, generating astrocyte stem trees through various options, and simulating the nanoscopic processes within the MSASTRO system.[7] Stem trees were selected from libraries, generated with endfoot structures, or loaded from reconstructed files. Nanoscopic process geometry was determined using default statistics or built-in tools. Parameters for membrane conductance and dendritic geometry were adjusted for accurate simulations. The resulting astrocyte models were compared to empirical data, and their morphology was refined to achieve alignment. Computer simulations were used to analyze sodium uptake mechanisms, focusing on the electrochemical properties of astrocytes and the Na^+, K^+-ATPase (Figure 2).

High-affinity Ca^{2+} indicators were employed to translate fluorescence signals into intracellular Ca^{2+} dynamics, requiring in-silico modeling of Ca^{2+} entry, diffusion, and buffering mechanisms. The clustering of Ca^{2+} channels was studied to reveal spatial dynamics and the role of channel clusters in Ca^{2+} signaling (Figure 3).

Architectural characteristics of astroglia were investigated through the examination of tissue volume fraction

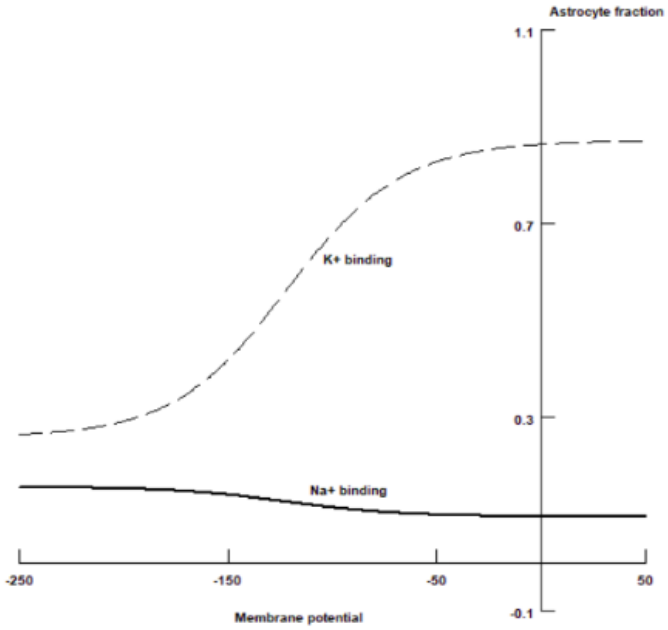

FIGURE 2. Summed distribution of astrocyte intermediate forms binding Na^+ and K^+ versus membrane potential.

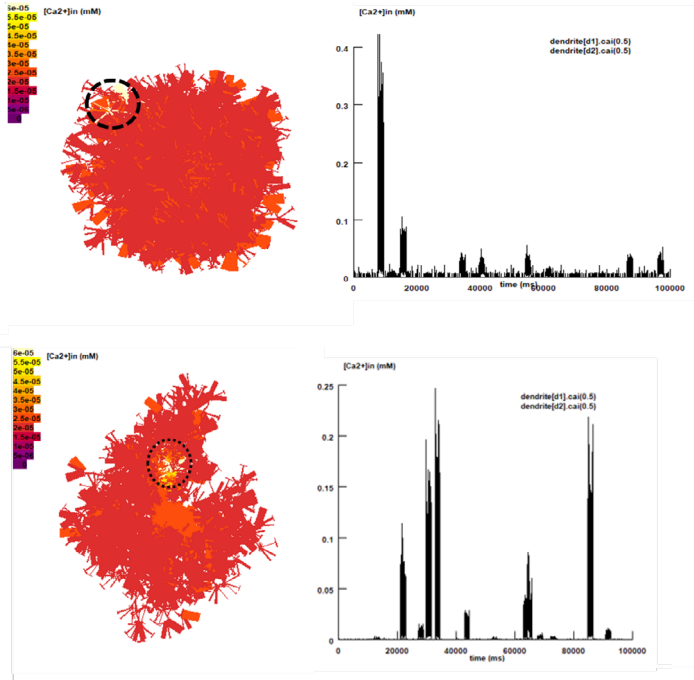

FIGURE 3. The visualization of the internal dynamics of Ca^{2+} in a cell is done through the use of dendrites. The black circle shows the area of interest, while the right shows the dendrites' d1 and d2.

(VF) and surface-to-volume ratios (SVR), providing insights into morphology and interactions with the surrounding environment (Figure 4). Computational modeling of cytokine signaling was conducted, focusing on interactions between microglial cytokines and their effects on astroglial behavior. Using an ordinary differential equation (ODE) model (Equation 1), the research explored the effects of autocrine/paracrine microglial cytokine interactions, particularly those involved MS, such as TNFα, IL-1β, and IL-6. We used a classic S-systems model formulation to simulate the expression dynamics of each cytokine (Figure 5a).

$$\frac{dC_x}{dt} = k_x f(C_i) f(C_j) - \gamma_x C_x - \gamma_{ss,x} C_{ss,x} \quad (1)$$

$$f(C_i) = \prod_i \frac{C_i(t-\tau_{d,ix})^{n_{ix}}}{C_i(t-\tau_{d,ix})^{n_{ix}} + K_{ix}^{n_{iz}}} \quad (2)$$

$$f(C_j) = \prod_j \frac{C_j(t-\tau_{d,jx})^{n_{jx}}}{C_j(t-\tau_{d,jx})^{n_{jx}} + K_{jx}^{n_{jz}}} \quad (3)$$

$$C_{ss,x} = C_x(t=0) \quad (4)$$

$$\gamma_{ss,x} = \frac{k_x f(C_i) f(C_j) - \gamma_x C_x}{C_{ss,x}} \quad (5)$$

where $C_x = C_x(t)$ is the expression of cytokine x (TNFα, IL-1β, IL-6) that is produced at rate k_x upon activation by cytokine C_i at time = $t - \tau_{d,ix}$. Thus the delay term $\tau_{d,ix}$ is time between the activation of C_i and its subsequent activation of C_x. The activation of C_x depends on C_i according to a Hill function characterized by half-maximal activation constant K_{ix} and cooperativity coefficient n_{ix}. Similarly, inhibitory cytokine C_j reduces C_x production with time delay $\tau_{d,jx}$ according to a decreasing sigmoidal function characterized by K_{jx} and n_{jx}. The degradation of C_x occurred with both concentration-dependent and concentration-independent components determined by rate constants γ_x and $\gamma_{ss,x}$, respectively. The concentration-independent degradation term encompassed the initial value of cytokine x, which was set to $C_{ss,x} = 0.1$ for all cytokines, and a degradation constant that was set to maintain a constant steady state [17] in the absence of stimulation.

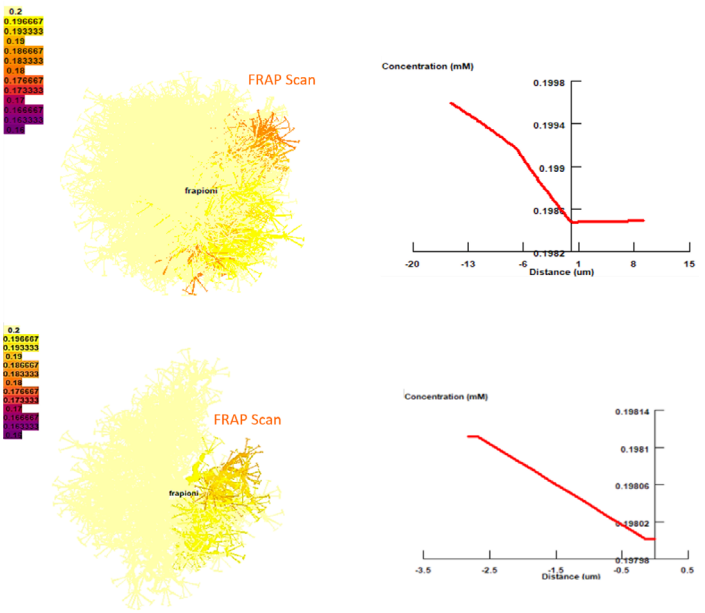

FIGURE 4. NEURON-based astrocyte model: determining volumetric quantities.

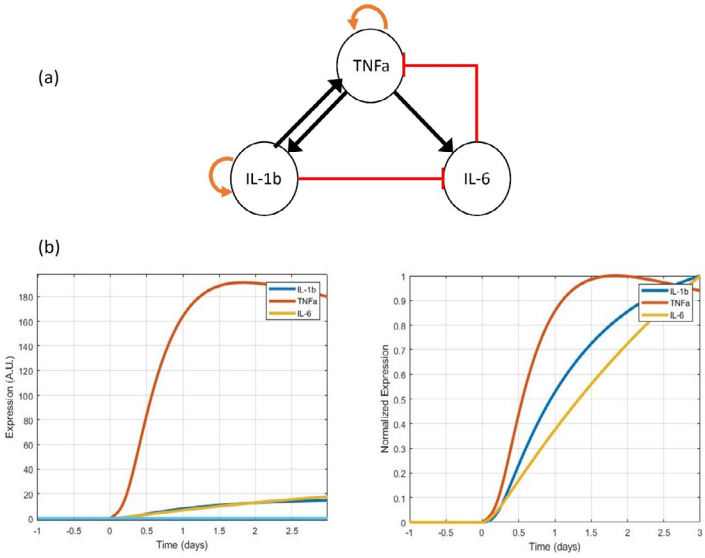

FIGURE 5. Network model and mathematical simulation of complex signaling dynamics cytokines. (a) The literature-based network model depicts the activation and inhibition of cytokine production. (b) The results of our calibrated model are shown along with a saturating stimulus of LPS = 1000 & t = 0.

Lastly, the study explored the requirements for effective conduction within astroglia particularly the influence of internodal distance on conduction velocity, and assessed the impact of parameters like Na^+ and K^+ channel density

on conduction. In astroglia, ion dynamics is a relatively slow process and the simulation trial normally requires needs at least 100 seconds.

RESULTS AND DISCUSSION

The results showcased that the chosen rate coefficients for isolated astrocytes and the current-voltage (I-V) relation were consistent with the physiological implications of the electrogenic sodium pump. This provided a fundamental understanding of sodium dynamics in these cells (Figure 2). No step involving binding or dissociation between Na^+ or K^+ and the astrocytes is directly influenced by voltage. There is a considerable indirect effect of voltage on the binding of Na^+ or K^+ to the astrocytes, owing to the voltage-dependent distribution of intermediates. Moving beyond sodium uptake, the research delved into the intricate world of astroglial calcium waves. While traditionally, slow global calcium elevations were the primary indicators of astroglial activity, recent advancements in high-sensitivity Ca^{2+} imaging revealed faster and more localized Ca^{2+} signals prevalent in smaller processes (Figure 3). The VF, which describes the proportion of local tissue occupied by astrocytes, was examined to provide insights into astrocyte morphology. Similarly, the SVR, a key biophysical determinant of a cell's function, was analyzed to evaluate how astrocyte morphology aligns with its surrounding environment. It is not known how SVR ranges in neocortex astroglial cells. However, we decided to evaluate surface area-to-volume ratios, which can be considered a measure of how much the morphology of a cell is adapted to interact with its environment. (Tables 1 and 2) ($SVR_{physiology}$ = 4.205 μm^{-1} & $SVR_{pathology}$ = 1.977 μm^{-1}). This provided quantitative data that shed light on the physical interact interactions between astrocytes and their surroundings (Figure 4).

The model provided insights into how these cytokines may influence astroglial responses under pathological conditions, paving the way for a deeper understanding of complex cellular interactions (Figure 5). By focusing on incorporating relevant mechanisms into the model, the study aimed to explore the requirements for effective conduction within astroglia. Notably, experimental evidence suggests a low Na^+ channel density within the internodal axolemma (2–6%), potentially acting as a mediator between demyelinated regions. Several simulations were conducted to scrutinize this possibility. In constructing the model, a 12-node axon was designed, with each node divided into regions representing demyelinated or remyelinated phases. The presence of new Ranvier nodes emerged in internodal regions during remyelination, creating short internodes. As the remyelination process progressed and the lamellae increased, the likelihood of successful Ranvier conduction escalated rapidly, although the conduction velocity remained low.

The relationship between internodal conduction time (ICT) and velocity exhibited a linear trend for small and large internodal lengths (L), with the increase in velocity observed only for L below 2000 µm (Figure 6). This study suggests the significance of internodal distance in conduction velocity and emphasizes the delicate balance between nodal and internodal currents for effective propagation.

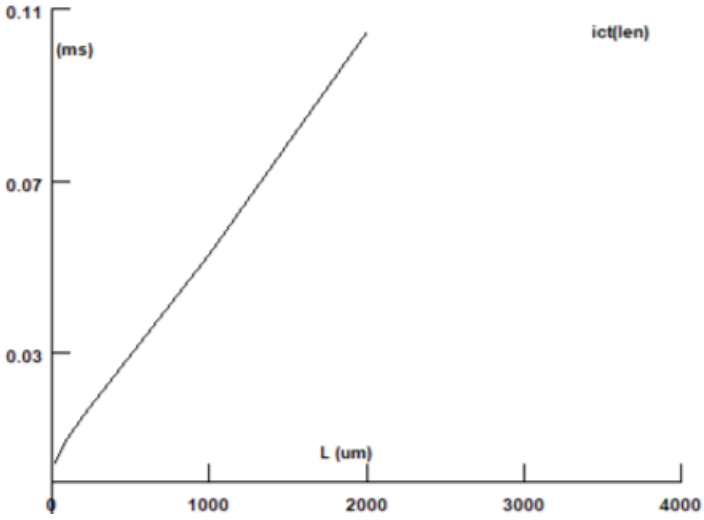

FIGURE 6. NEURON-based astrocyte model: determining volumetric quantities.

CONCLUSION

In summary, this study uses advanced computational modeling to explore astroglial physiology and interactions, providing insights into astrocyte function, calcium dynamics, tissue architecture, and cytokine signaling. It raises questions about how specific inflammatory stimuli influence disease outcomes and whether modulating

astrocyte responses could have therapeutic potential. The study emphasizes the need for comprehensive frameworks like S-systems to understand cytokine interactions and their impact on targets, offering a promising avenue for deeper understanding and potential intervention in neurological disorders.

ACKNOWLEDGMENT

This work was based on ASTRO by the Department of Clinical and Experimental Epilepsy, Institute of Neurology, University College of London. The authors thank Dr. Leonid Savtchenko for his inspirational support.

REFERENCES

1. Ravi, K., Paidas, M.J., Saad, A., et al. Astrocytes in rare neurological conditions: Morphological and functional considerations. *J Comp Neurol.* 2021;529(10):2676–2705. https://doi.org/10.1002/cne.25118.
2. KPonath, G., Park, C., Pitt, D. The Role of Astrocytes in Multiple Sclerosis. *Front Immunol*. 2018;9:217. https://doi.org/10.3389/fimmu.2018.00217.
3. Henstridge, C.M., Tzioras, M., Paolicelli, R.C. Glial Contribution to Excitatory and Inhibitory Synapse Loss in Neurodegeneration. *Front Cell Neurosci*. 2019;13(63). https://doi.org/10.3389/fncel.2019.00063.
4. Carlos, R., Gustavo, S., Gaston, K., et al. Brain atrophy in Multiple Sclerosis. *Am J Psychiatry Neurosci*. 2015;3(3):40–49. https://doi.org/10.11648/j.ajpn.20150303.11.
5. Correale, J., and Farez, M.F. The Role of Astrocytes in Multiple Sclerosis Progression. *Front Neurol*. 2015; 6(180). https://doi.org/10.3389/fneur.2015.00180.
6. Wheeler, M.A. and Quintana, F.J. Regulation of Astrocyte Functions in Multiple Sclerosis. *Cold Spring Harb Perspect Med*. 2019;9(1):a029009. https://doi.org/10.1101/cshperspect.a029009.
7. Savtchenko, L.P., Bard, L., Jensen, T.P., et al. Disentangling astroglial physiology with a realistic cell model in silico. *Nat Commun*. 2018;9(1):3554. https://doi.org/10.1038/s41467-018-05896-w. Erratum in: *Nat Commun*. 2019; 10(1):5062. https://doi.org/10.1038/s41467-019-12712-6.
8. Batiuk, M.Y., Martirosyan, A., Wahis, J., et al. Identification of region-specific astrocyte subtypes at single cell resolution. *Nat Commun*. 2020;11(1):1220. https://doi.org/10.1038/s41467-019-14198-8.
9. Rusakov, D.A., Bard, L., Stewart, M.G., et al. Diversity of astroglial functions alludes to subcellular specialisation. *Trends Neurosci*. 2014;37(4):228-42. https://doi.org/10.1016/j.tins.2014.02.008.
10. Savtchenko, L.P. and Rusakov, D.A. Regulation of rhythm genesis by volume-limited, astroglia-like signals in neural networks. *Philos Trans R Soc Lond B Biol Sci*. 2014; 369(1654):20130614. https://doi.org/10.1098/rstb.2013.0614.
11. Schiweck., J., Eickholt, B.J., Murk, K. Important Shapeshifter: Mechanisms Allowing Astrocytes to Respond to the Changing Nervous System During Development, Injury and Disease. *Front Cell Neurosci*. 2018;12(261). https://doi.org/10.3389/fncel.2018.00261.
12. Zhou, B., Zuo, Y.X., Jiang, R.T. Astrocyte morphology: Diversity, plasticity, and role in neurological diseases. *CNS Neurosci Ther.* 2019;25(6):665–673. https://doi.org/10.1111/cns.13123.
13. Clavreul, S., Abdeladim, L., Hernández-Garzón, E., et al. Cortical astrocytes develop in a plastic manner at both clonal and cellular levels. *Nat Commun*. 2019; 10(1):4884. https://doi.org/10.1038/s41467-019-12791-5.
14. Fleidervish, I., Lasser-Ross, N., Gutnick, M., et al. Na^+ imaging reveals little difference in action potential–evoked Na^+ influx between axon and soma. *Nat Neurosci*. 2010;13(7):852–860. https://doi.org/10.1038/nn.2574.
15. Hines, M. and Shrager, P. A computational test of the requirements for conduction in demyelinated axons. *Restor Neurol Neurosci*. 1991;3(2):81–93. https://doi.org/10.3233/RNN-1991-3205.
16. Carnevale, N.T. and Hines, M.L. The NEURON Book; Cambridge UP: Cambridge, UK; 2006.
17. Furchtgott, L.A., Chow, C.C., Periwal, V. A Model of Liver Regeneration. *Biophys J*. 2009;96(10):3926–3935. https://doi.org/10.1016/j.bpj.2009.01.061.